Radiative Forcing and Global Temperatures: 800,000 Years of Co-Movement*

Marc Gronwald†
Xin Jin‡
Sania Wadud§

December 2024
VERY PRELIMINARY DRAFT

Abstract

This paper evaluates paleoclimate sensitivity over the past 800,000 years using two recently proposed co-movement measures: Long-run covariability and quantile coherency. The former allows one to calculate long-run correlation as well as long-run regression coefficients. The latter is based on cross-spectral densities; it characterizes the dependence in quantiles of the joint distribution across frequencies. Both allow one to focus on long-term components of the data; this addresses the uncertainty associated with paleoclimatic reconstructions of radiative forcings as well as temperatures. The long-run correlation coefficient and long-run regression coefficient are found to be 0.87 and 0.76, respectively. The quantile coherency analysis finds that the dependence is generally stronger for the long-term components of the data, but also significantly lower in smaller quantiles of the joint distribution of temperatures and forcing. Thus, the relationship is weaker during full glacial climates compared to interglacial periods and intermediate glacial climates.

Keywords: Climate change, Paleoclimatic data, Global temperature reconstruction, Radiative forcing, Long-run covariability, Quantile

*The authors are grateful to participants at the Climate Econometric Seminar, in particular Zack Miller, David Hendry, and Francis Diebold, the 2024 Australasian Meeting of the Econometrics Societyas well as the 2024 NAERE workshop for valuable feedback.

†International Business School Suzhou, Xi'an Jiaotong-Liverpool University; CESifo and ifo Institute. Email: marc.gronwald@xjtlu.edu.cn.

‡Duke Kunshan University and University of Aberdeen

§University of Leeds

coherency
JEL-Classification: C32, Q54

1 Introduction

This paper is concerned with an evaluation of paleoclimate sensitivity over the past 800,000 years. It uses proxy-based reconstructions of changes in global temperatures, ice sheets and sea level, vegetation, dust, and greenhouse gases (Snyder, 2016; Snyder 2019). Snyder (2019) finds the relationship between ΔT and ΔR to be non-linear.[1] This paper applies two methods to further analyse this relationship: first, Baruník and Kley's (2019) quantile coherency; a general measure for dependence between cyclical variables. Second, Mueller and Watson's (2018) covariability; based on this, a long-run correlation coefficient and long-run linear regression coefficient can be calculated.

To provide the general background for this research, climate sensitivity measures the change in global temperatures in response to changes in radiative forcing. The existing literature identified four key components of climate sensitivity: (1) climate state, (2) stimuli of global temperature response, (3) scope of included feedback, (4) time frame of response. A more specific concept used is the so-called equilibrium climate sensitivity (ECS): the equilibrium global average surface temperature change in response to a doubling of the atmospheric concentration of carbon dioxide from preindustrial levels (IPCC, 2013). The estimation of ECS requires climate model as this allows controls which feedbacks are "turned on". Snyder (2019), however, points out that the Climate system is constantly evolving, is never at equilbrium, and that multiple feedbacks are active across multiple timescales.

In the context of the study of past climates, the precise definition of ECS is not applicable. Commonly applied is the notion of "specific climate sensitivity": this is the ratio between deviations in global temperature from the present state and deviations in radiative forcing from the present state (Rohling et al., 2012)). Snyder (2019) estimates the so-called "paleoclimate sensitivity parameter" $S_{[GHG,LI,AE,VG]}$ which measures the change in global mean surface air temperature ΔT is function of change in radia-

[1] Note that ΔT and ΔR denotes the change in temperatures and forcing compared to a recent benchmark.

tive perturbation$\Delta R_{[GHG,LI,AE,VG]}$ multiplied by $S_{[GHG,LI,AE,VG]}$. The key difference of $S_{[GHG,LI,AE,VG]}$ and ECS: $S_{[GHG,LI,AE,VG]}$ is a functional relationship between two interactive time series, not an equilibrium response to a specific single forcing. Analyses of paleoclimate reconstructions estimate relationships between different climate variables without identifying causation. Multiple changes likely interacted with each other to drive climate changes over the past million years (Snyder, 2019).

Previous paleoclimate sensitivity research focused on reconstructing single points in time, such as the Last Glacial Maximum (Edwards, Crucifix, & Harrison, 2007); recently, however, the investigation of paleoclimate sensitivity using time series from the paleoclimate record became more common (Friedrich, Timmermann, Tigchelaar, Timm, & Ganopolski, 2016; Rohling et al., 2012). In particular, paleoclimate sensitivity is estimated by performing regression analyses on time series of paleoclimate reconstructions of ΔT and ΔR. It is important to note that ΔR is obtained from changes in ice sheets, atmospheric dust, and vegetation are estimated using paleoclimate reconstruction and that these reconstructions are scaled to ΔR using estimates of change in ΔR at the Last Glacial Maximum.

Worth mentioning are also analyses of paleoclimate data using traditional econometric methods: Kaufmann and Juselius (2010) analyse the role of orbital, seasonal, and spatial variations within glacial cycles; the same authors also test hypotheses about the physical mechanisms that may drive glacial cycles (Kaufmann & Juselius, 2013). Davidson, Stephenson, and Turasie (2016) are among the first to use methods such as Granger causality to analyse paleoclimate data. Kaufmann and Pretis (2018) propose a statistical climate model of 800,000 years of data, and Miller (2019) is testing cointegration relationships among irregular and non-contemporaneous series - a common issue in the context of paleoclimate data. Adrian et al. (2022), finally, are concerned with the analysis of 800,000 years of climate risk.[2]

Having explained the background of this paper, the focus is now directed to the data which is displayed in Figure 1. The solid lines represent the median estimates for global temperatures and radiative forcing, the shaded

[2]For a more general discussion, see Castle and Hendry (2020).

areas are the 95% confidence interval. They reflect the uncertainty associated with the reconstructions.

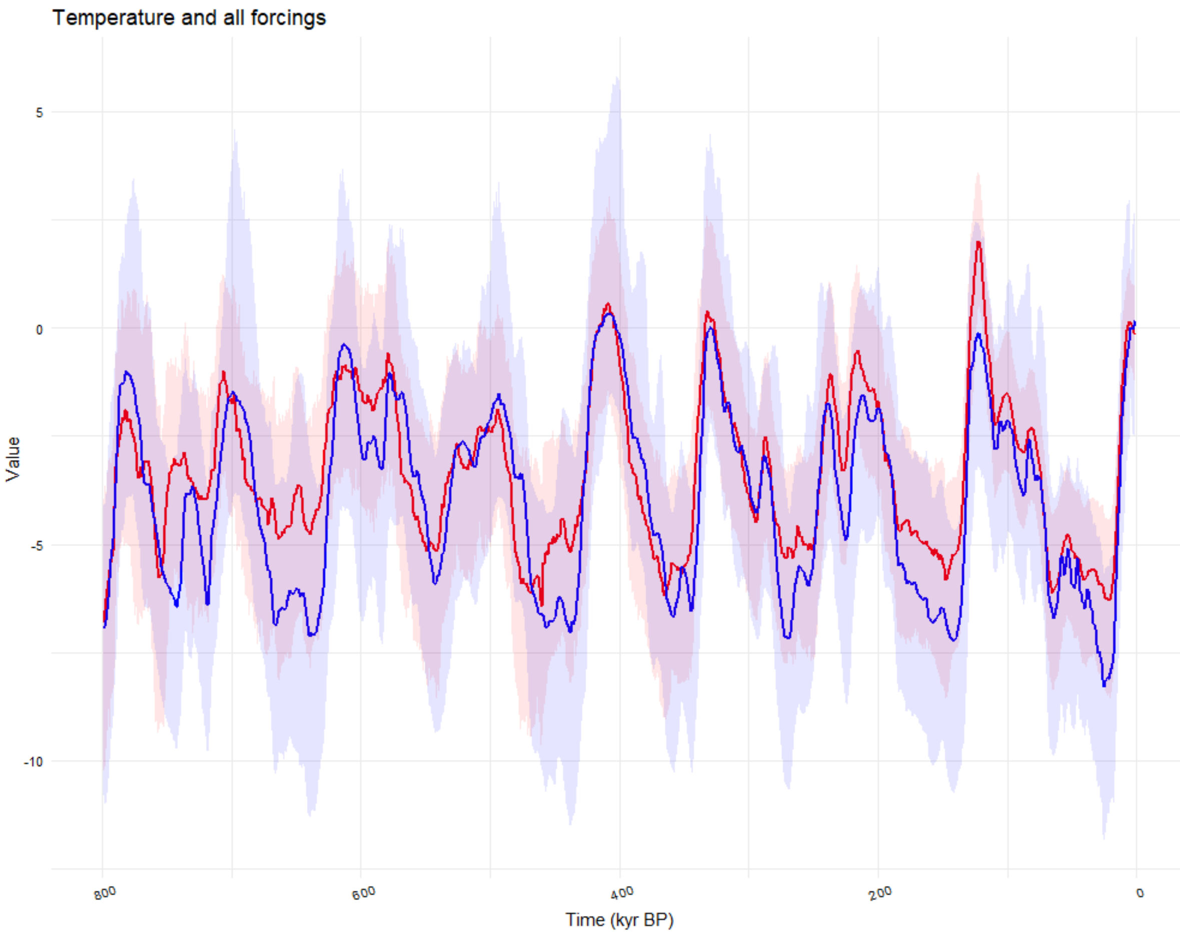

Figure 1: Reconstructions of $\Delta R (W/m^2)$ and $\Delta T (^{\circ}C)$

It is evident that both series exhibit a very strong cyclical pattern. The relationship generally appears to be strong; on many occasions turning points of the series occur at the same time. At the same time, there are also frequent deviations of the series from each other. Note that the data frequency is 1k years and that time is denoted as k years before present (BP).

This data is from Snyder (2016) as well as Snyder (2019). The former provides a spatially weighted proxy reconstruction of global temperature over the past 2 million years estimated from a multiproxy database of over 20,000 sea surface temperature point reconstructions. The contribution of the latter lies in a quantification of sources of uncertainty in estimating ΔR. The statistical methods Snyder (2019) applies are not biased by the variable (heteroscedastic) uncertainty in the reconstructions. That paper applies a Monte Carlo-style probabilistic framework. The main empirical results of Snyder (2019) can be summarised as follows: a strong comovement of ΔR and ΔT over last 800,000 years is found; the correlation is 0.81 (credible interval 0.6 to 0.9). Worth highlighting is that there is a lower correlation and lower responsiveness at colder temperatures: Paleoclimate sensitivity parameter estimate: $0.84°C/W/m^2$ (interglacial periods, intermediate glacial climates) and $0.53°C/W/m^2$ (full glacial climates). Finally, Snyder (2019) provides evidence of time-varying correlation, but no time variation in sensitivity parameter estimate. These findings are based on a rolling window analysis.

As mentioned above, this paper uses two recently proposed co-movement measures to analyse this data. Baruník and Kley's (2019) quantile coherency allows one to capture complex dynamics of macroeconomic or financial time series. The motivation to put forward this method comes from the observation that extreme negative events in one asset can cause irrational outcomes in other assets. In addition, markets may be more strongly connected in extreme periods than in tranquil ones The long-term fluctuations in quantiles of joint distribution may differ from those in the short-term due to differing risk perceptions of agents over distinct investment horizons. The motivation for Mueller and Watson (2018) is related to the so-called Great Ratios: Economic theories often have stark predictions about the covariability of variables over long-horizons, which is often a proportional movement. According to the permanent income hypothesis, consumption and income are strongly related, long-run PPP predicts that nominal exchange rates and relative nominal prices move together in the long run. Note that the confidence bands for the long-run correlation coefficient and the long-run regression coefficient are valid for I(0), I(1), near unit roots, and fractionally integrated models.

The key findings are the following: long-run correlation coefficient and long-run regression coefficient are found to be 0.87 and 0,76, respectively. The quantile coherency analysis shows that the dependence is generally stronger for the long-term components of the data. However, the dependance is found to be significantly lower in smaller quantiles of the joint distribution of temperatures and forcing also for the long-term components. In other words, the relationship is considerably weaker during full glacial climates compared to interglacial periods and intermediate glacial climates. In short, the relationship between radiative forcing and temperatures over the past 800,000 years is highly complex.

The remainder of the paper is organised as follows: Section 2 presents empirical methods used in this paper, followed by a presentation of the results in Section 3. Section 4 offers some concluding remarks.

2 Empirical approaches

2.1 Long-run covariability

The first method this paper employs is the measure of long-run covariability proposed by Mueller and Watson (2018).[3] The main idea of this approach can be summarised as follows: centre stage takes a so-called low-pass transformation of a univariate time series $x_t, t = 1, \ldots, T$. The purpose of this transformation is the isolation of the variation in the series which exceeds a certain period. The length of this period is controlled by a parameter q. Cosine functions are used to capture these periodic functions: $\Psi_j(s) = \sqrt{2}\cos(js\pi)$ denotes these functions with period $2/j$.[4]

The outcome of this transformation is also referred to as low-frequency projection of x, denoted by $\hat{x}$. In order to analyse the long-run covariability of two variables (x, y), the relationship of the respective long-run projec-

[3] This paper only outlines this method. The original paper contains all methodlogical details.

[4] $\Psi(s) = [\Psi_1(s), \Psi_2(s), \ldots, \Psi_q(s)]'$ denotes a vector of these functions with periods 2 through $2/q$, and Ψ_T denote the $T \times q$ matrix with tth row given by $\Psi((t - 1/2)T)'$, so the jth column of Ψ has period $2T/j$.

tions $(\hat{x}, \hat{y})$ is evaluated. Ω_T denotes the average covariance matrix of those long-run projections in a sample of T. This (2x2) matrix summarises their variability and covariability. From that, the long-run correlation and long-run linear regression coefficient can be derived as follows:

$$\begin{aligned}
\rho_T &= \Omega_{xy,T}/\sqrt{\Omega_{xx,T}\Omega_{yy,T}}, \\
\beta_T &= \Omega_{xy,T}/\Omega_{xx,T}, \\
\sigma_{y|x,T} &= \Omega_{yy,T} - (\Omega_{xy,T})^2/\Omega_{xx,T},
\end{aligned} \tag{1}$$

where $(\Omega_{xx,T}, \Omega_{xy,T}, \Omega_{yy,T})$ are elements of Ω_T.

2.2 Quantile coherency

The second method this paper applies is Baruník and Kley's (2019) quantile coherency. As mentioned above, the method allows one to quantify the dependence between time series. A well-documented challenge in this regard is that, on the one hand, that strongly correlated variables are truly independent: Spurious correlation (Granger & Newbold, 1974). On the other hand, uncorrelated variables may possess dependence in different parts of joint distribution and/or at different frequencies. Neither linear correlation nor traditional cross-spectral methods can detect that type of complex relationship. Quantile coherency is based on cross-spectral densities: the method characterizes the dependence in quantiles of the joint distribution across frequencies. To be precise, dependence is quantified in terms of the probabilities to exceed quantiles.

Quantile coherency is a normalized version of the quantile cross-spectral density, analogous to traditional coherency in spectral analysis. The quantile cross-spectral density between two time series X_t and Y_t at quantiles τ_1 and τ_2, and at frequency ω, is given by:

$$f_{X,Y}(\tau_1, \tau_2, \omega) = \sum_{h=-\infty}^{\infty} \gamma_{X,Y}(\tau_1, \tau_2, h) e^{-i\omega h}$$

where $\gamma_{X,Y}(\tau_1, \tau_2, h)$ is the quantile cross-covariance at lag h, and ω is the frequency.

Quantile coherency can be is defined as:

$$qC_{X,Y}(\tau_1, \tau_2, \omega) = \frac{f_{X,Y}(\tau_1, \tau_2, \omega)}{\sqrt{f_{X,X}(\tau_1, \tau_1, \omega) f_{Y,Y}(\tau_2, \tau_2, \omega)}}$$

Here, $f_{X,X}(\tau_1, \tau_1, \omega)$ and $f_{Y,Y}(\tau_2, \tau_2, \omega)$ represent the quantile auto-spectral densities for X_t and Y_t, respectively.

The quantile coherency $qC_{X,Y}(\tau_1, \tau_2, \omega)$ provides information on the strength of dependence between the time series X_t and Y_t at quantiles τ_1 and τ_2, across different frequencies ω. This methodology extends classical coherency analysis by incorporating dependencies at different parts of the distribution, making it useful for analyzing relationships in both normal and extreme market conditions.

A MORE FORMAL DISCUSSION OF THE METHOD TO BE INCLUDED HERE

3 Results

This section summarises the main results. Table 1 displays the long-run covariability estimates including the confidence bands.[5] Note that the value for q has been chosen to be 16 initially.[6]

As the data is at 1k year frequency and there are 800 observations, this implies that the long-run projections used here represent periods longer than $\frac{2T}{q} = 2 * 800/16 = 100$k years. This falls into the range of periods Mueller and Watson (2018) use in their analysis of macroeconomic variables. Figure 2a shows these long-run projections. It is evident that the short-run fluctuations of both global temperatures and radiative forcing have been largely smoothed out. Figure 2b illustrates the effect of choosing different

[5] These results have been obtained from the application of the so-called A,B,c,d-Model; see Mueller and Watson (2018) for details. This paper uses the original replication code.

[6] The setting of this parameter reflects, according to Mueller and Watson (2018) what the researcher believes the long-run is. The interested reader is referred to the detailed discussion in the original paper.

Table 1: Long-run covariablity estimates and confidence intervals

	q=16		
	ρ	β	$\sigma_{y\|x}$
Estimate	0.87	0.74	0.65
67% CI	0.75, 0.92	0.63, 0.84	0.55, 0.79
90% CI	0.64, 0.95	0.55, 0.92	0.49, 0.93
67% Bayes CS	0.78, 0.92	0.63, 0.84	0.55, 0.79
90% Bayes CS	0.64, 0.95	0.55, 0.92	0.49, 0.93
	q=20		
	ρ	β	$\sigma_{y\|x}$
Estimate	0.87	0.76	0.69
67% CI	0.80, 0.92	0.67, 0.85	0.59, 0.82
90% CI	0.75, 0.95	0.60, 0.92	0.53, 0.95
67% Bayes CS	0.85, 0.92	0.67, 0.85	0.59, 0.82
90% Bayes CS	0.75, 0.95	0.60, 0.92	0.53, 0.95

setting for the parameter q: the larger q, which corresponds to using shorter periods, the larger the extent of short-run fluctuations that remains in the data.

The long-run correlation coefficient is estimated to be 0.87; the long-run regression coefficient 0.74. The confidence bands for both do not include 0. This implies that there is a significant long-run relationship between global temperatures and radiative forcings. As illustrated above, the two series under consideration exhibit a strong cyclical pattern, but both reconstructions are associated with considerable uncertainty. Smoothing out the short-term fluctuation is one way to deal with this issue. For this reason, it is useful to consider additional values for q. While $q = 16$ captures periods longer than 100,000 years, for $q = 20$, those are longer than $2 * 800/20 \approx 80,000$ years. The long-run correlation coefficient is estimated to be 0.87 in this case as well; also the estimate of the long-run regression coefficient is not strongly affected. Note that Mueller and Watson (2018) analyse a number of macroeconomic relationships using this method. To name just two, they find the long-run correlation coefficient of GDP growth and consumption

Figure 2: Long-run projections of global temperatures and radiative forcing

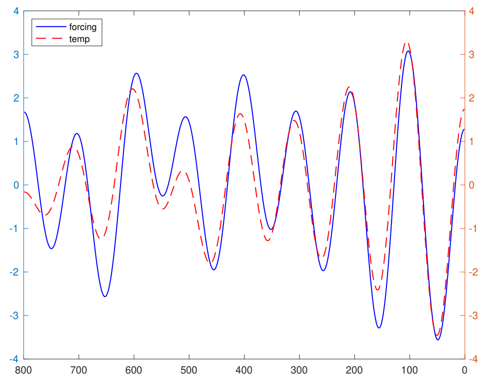

(a) $q = 16$

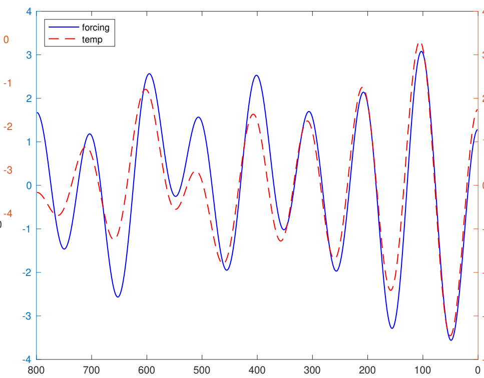

(b) $q = 20$

growth to be 0.91 and that of short- and long-term interest rates to be 0.96. Thus, the long-run correlations found in this paper fall roughly into the range typically found in macroeconomic applications of this method.

Figure 3 shows the results from the application of Baruník and Kley's (2019) quantile coherency. As this method focusses on dependence in quantiles of the joint distribution of the data, it is important to highlight that the lower quantiles capture those periods in which both series take small values. This generally includes the colder periods or the (deep) glacial conditions. Warmer periods such as intermediate glacial conditions and interglacial periods would be captured by the upper quantiles of the joint distribution. The left panel of the figure shows the coherency at the 50% quantile (median), the 5% quantile as well as the 95% quantile of the joint distribution of temperatures and forcing. The following general pattern emerges: the dependence is found to be considerably stronger for the long-term components of the series than for the short-term ones. In addition, and more importantly, cycles at the lower quantiles appear to be much weaker dependent than those at the upper quantiles. In other words, in colder periods,

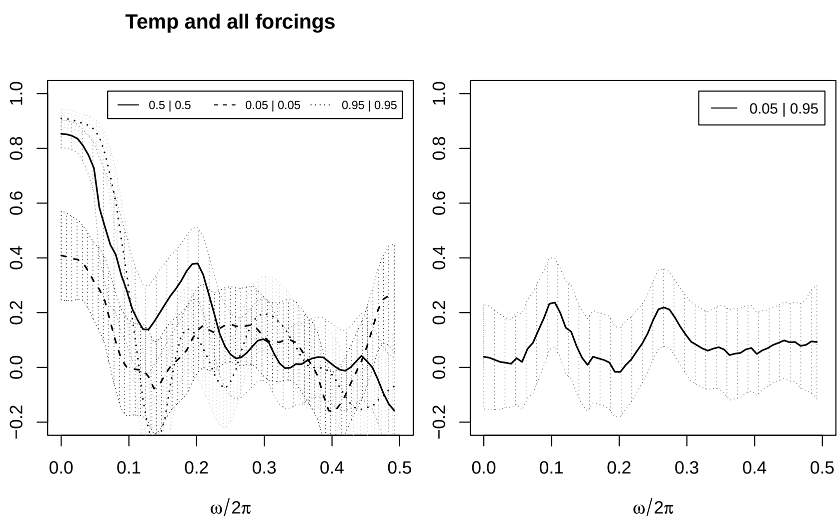

Figure 3: Barunik and Kley's (2019) quantile coherency

the relationship between the series is much weaker. This finding is generally consistent with Snyder (2019), but it is remarkable that also the dependence of the long-term components is weaker.

Snyder (2019) further evaluates the correlation of global temperatures and radiative forcing as well as the paleoclimate sensitivity parameter using a rolling window approach. The remarkable finding is that there is some evidence of time-variation in the correlation, but not in the sensitivity parameter. To look into this issue, this paper splits the sample into an early and a late subsample. Figure 4 shows the quantile coherency estimates for these two subsamples. It is evident that there is a stark difference: in the early sample, there is a considerable difference in the dependence across quantiles - the pattern is more pronounced than in the full sample: the dependence is the strongest for the upper quantiles and the weakest for the lower quantiles. In this case, there is a difference also between the dependence at the upper quantiles and the median. As for the late subsample, the differences in dependence across quantiles is found to be much smaller: now also at lower quantiles a strong dependence is found for the long-term

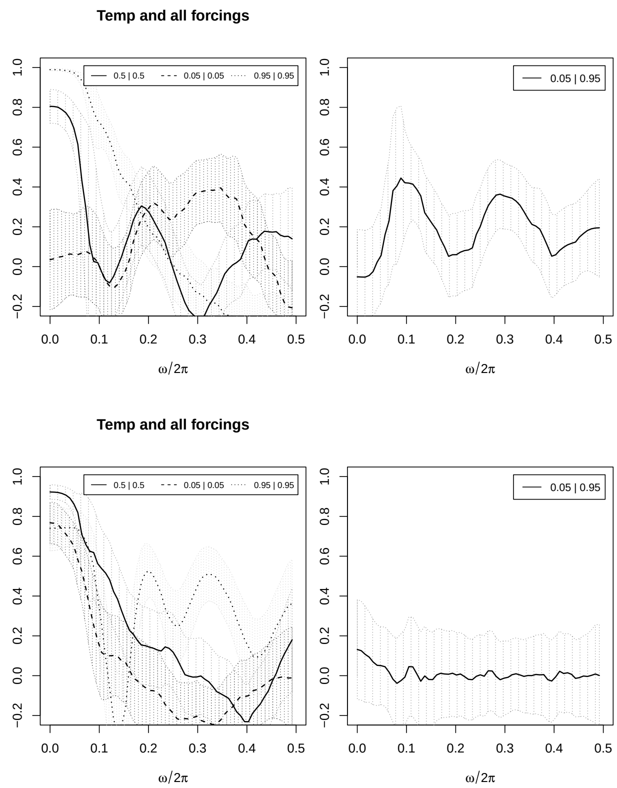

Figure 4: Barunik and Kley's (2019) quantile coherency - early subsample (upper panel), late subsample (lower panel)

components of the data.

4 Concluding remarks

The analysis of paleoclimate sensitivity is concerned with the relationship between global temperatures and radiative forcing. Both variables are based on reconstructions. There is uncertainty associated with these reconstructions. The methods used in this paper, long-run covariablity as well quantile coherency, allow one to analyse the co-movement of time series across frequencies and periods, respectively. Thus, some of this uncertainty has been smoothed out. In addition, the existing literature on paleoclimate sensitivity, in particular Snyder (2019), finds that there is a non-linear relationship between global temperatures and radiative forcing. Baruník and Kley's (2019) quantile coherency in particular allow one to analyse complex dependence structures between time series.

The key findings are the following: the long-run correlation coefficient and long-run regression coefficient are found to be 0.87 and 0,76, respectively. The quantile coherency analysis shows that the dependence is generally stronger for the long-term components of the data. However, the dependance is found to be significantly lower in smaller quantiles of the joint distribution of temperatures and forcing also for the long-term components. In other words, the relationship is considerably weaker during full glacial climates compared to interglacial periods and intermediate glacial climates. In short, the relationship between radiative forcing and temperatures over the past 800,000 years is highly complex.

References

Adrian, T., Boyarchenko, N., Giannone, D., Prasad, A., Seneviratne, D., & Xiao, Y. (2022). *800 , 000 Years of Climate Risk* (No. 1031). (Federal Reserve Bank of New York Staff Reports No 1031)

Baruník, J., & Kley, T. (2019). Quantile coherency: A general measure for dependence between cyclical economic variables. *Econometrics Journal*, *22*(2), 131–152. doi: 10.1093/ectj/utz002

Castle, J., & Hendry, D. (2020). Identifying the causal role of co2 during the ice ages.

Davidson, J. E., Stephenson, D. B., & Turasie, A. A. (2016). Time series modeling of paleoclimate data. *Environmetrics*, *27*(1), 55–65. doi: 10.1002/env.2373

Edwards, T. L., Crucifix, M., & Harrison, S. P. (2007). Using the past to constrain the future: How the palaeorecord can improve estimates of global warming. *Progress in Physical Geography*, *31*(5), 481–500. doi: 10.1177/0309133307083295

Friedrich, T., Timmermann, A., Tigchelaar, M., Timm, O. E., & Ganopolski, A. (2016). Nonlinear climate sensitivity and its implications for future greenhouse warming. *Science Advances*, *2*(11). doi: 10.1126/sciadv.1501923

Granger, C. W., & Newbold, P. (1974). Spurious regressions in econometrics. *Journal of econometrics*, *2*(2), 111–120.

Kaufmann, R. K., & Juselius, K. (2010). Glacial cycles and solar insolation: the role of orbital, seasonal, and spatial variations. *Climate of the Past Discussions*, *6*(6), 2557–2591. Retrieved from `http://www.clim-past-discuss.net/6/2557/2010/` doi: 10.5194/cpd-6-2557-2010

Kaufmann, R. K., & Juselius, K. (2013). Testing hypotheses about glacial cycles against the observational record. *Paleoceanography*, *28*(1), 175–184. doi: 10.1002/palo.20021

Kaufmann, R. K., & Pretis, F. (2018). *Out-of-Sample Paleo-Climate Simulations: Testing Hypothesis About the Mid-Brunhes Event, the Stage 11 Paradox, and Orbital Variations* (No. April). (University of Victoria Discussion Paper)

Miller, J. I. (2019). Testing Cointegrating Relationships Using Irregular and Non-Contemporaneous Series with an Application to Paleoclimate Data. *Journal of Time Series Analysis*, *40*(6), 936–950. doi: 10.1111/jtsa.12469

Mueller, U. K., & Watson, M. W. (2018). Long-run covariability. *Econometrica*, *86*(3), 775–804.

Rohling, E. J., Sluijs, A., Dijkstra, H. A., Köhler, P., Van De Wal, R. S., Von Der Heydt, A. S., ... Zeebe, R. E. (2012). Making sense of palaeoclimate sensitivity. *Nature*, *491*(7426), 683–691. Retrieved from `http://dx.doi.org/10.1038/nature11574` doi: 10.1038/nature11574

Snyder, C. W. (2016). Evolution of global temperature over the past two million years. *Nature*, *538*(7624), 226–228. Retrieved from `http://dx.doi.org/10.1038/nature19798` doi: 10.1038/nature19798

Snyder, C. W. (2019). Revised estimates of paleoclimate sensitivity over the past 800,000 years. *Climatic Change*, *156*(1-2), 121–138. doi: 10.1007/s10584-019-02536-0